Macrophage-stimulating activities of newly isolated complex polysaccharides from *Parachlorella kessleri* strain KNK-A001

Mikinori Ueno[a], Kichul Cho[b], Narumi Hirata[a], Kenji Yamashita[c], Kenichi Yamaguchi[a], Daekyung Kim[d*] and Tatsuya Oda[a*]

[a]*Graduate School of Fisheries Science and Environmental Studies, Nagasaki University, 1-14 Bunkyo-machi, Nagasaki, Nagasaki 852-8521, Japan*

[b]*Geum River Environment Research Center, National Institute of Environmental Research, Jiyong street, Okcheon gun, Chungcheongbuk do 373-804, Republic of Korea*

[c]*KANEKA Corporation, 2-3-18 Nakanoshima Kita-Ku, Osaka 530-8288, Japan*

[d]*Jeju center, Korea Basic Science Institute (KBSI), Smart Building 1F, Jeju Science Park, 2170-2, Ara-dong, Jeju-Si, Jeju Special Self-Governing Province 690-756, Republic of Korea*

* Corresponding authors. Fax: +81-95-819-2831. *E-mail address*: dkim@kbsi.re.kr (D. Kim) and t-oda@nagasaki-u.ac.jp (T. Oda)

Highlights

Parachlorella kessleri strain KNK-A001 has various water-soluble polysaccharide fractions with different bioactivities.

The water-soluble polysaccharides can be separated into five fractions by DEAE anion exchange chromatography.

F5, a fraction isolated from *Parachlorella kessleri* strain KNK-A001, shows the most potent induction of the secretion of NO and TNF-α from RAW264.7 cells.

The activity of F5 is mediated through the activation of NF-κB.

MAP kinase signalling pathways are involved in the macrophage-stimulating activities of F5.

Key words: *Parachlorella kessleri*, polysaccharides, Macrophages, Nitric oxide, TNF-α, NF-κB

Abstract

Our previous studies demonstrated that the microalga *Parachlorella kessleri* (KNK-A001) has immunostimulatory activities, which were observed as an increase in natural killer (NK) cell activity in mice after intraperitoneal injection or as a protective effect on a virus-infected model shrimp after oral administration. In this study, we attempted to gain insight into the constituent substances of KNK-A001 that are responsible for the immunostimulatory activity. First, we obtained five polysaccharide fractions from KNK-A001 by DEAE anion exchange chromatography. Among the fractions, F5 showed the most potent induction of nitric oxide (NO) secretion in RAW264.7 cells, and both mRNA and protein expression levels of inducible NO synthase (iNOS) were increased in F5-treated RAW264.7 cells. A significant increase in the nuclear translocation of the p65 subunit of nuclear factor-kappa B (NF-κB) was observed in F5-treated RAW264.7 cells. F5 also induced the secretion of tumour necrosis factor (TNF)-α in RAW264.7 cells. Analysis using mitogen-activated protein (MAP) kinase inhibitors suggested that c-Jun N-terminal kinase (JNK) and p38 MAP kinase were mainly involved in F5-induced NO and TNF-α productions. The compositional analysis of F5 identified the main constituents as galactose, glucose, galacturonic acid, and mannose. Gel-filtration analysis suggested that molecular mass of F5 was approximately 400 kDa.

1. Introduction

The *Parachlorella kessleri* strain KNK-A001 is a green microalga taxonomically similar to *P. kessleri.* Although the microscopic morphological features of this microalga are indistinguishable from those of *Chlorella vulgaris*, it has a thick extracellular matrix that consists of polysaccharides, instead of the hard cell wall observed in *C. vulgaris*. In the course of our study to identify the functions of KNK-A001, we found that dry powdered KNK-A001 was a good value food for the Pacific oyster spat and the zooplankton rotifer *Brachionus plicatilis* [1]. Faecal analysis suggested that this was partly attributed to the easier digestion of KNK-A001 in those organisms compared with *C. vulgaris*, rather than to differences in nutrient value. Recent studies showed that the intraperitoneal injection of a KNK-A001 cell suspension into mice resulted in a significant increase in splenic natural killer (NK) cell activity against YAC-1 cells; the activity was much higher than that induced by *C. vulgaris*. Hence, it was suggested that KNK-A001 has potent *in vivo* immunostimulatory activity [2].

Kuruma shrimp (*Marsupenaeus japonicus*) is one of the most important aquatic organisms of aquacultural food resources in Japan. However, the farming of kuruma shrimp, as well as other commercially cultured shrimp species, has been severely impacted by white spot syndrome virus (WSSV) infection, which can cause almost complete mortality in the shrimp species within a few days of infection and often results in serious economic losses. As crustaceans do not have an acquired immune system, one of the most effective strategies for prophylaxis and the control of viral infections is the use of immunostimulants to activate the innate immune system. Consequently, the immunostimulatory effects of various substances, such as peptidoglycan, lipopolysaccharides, glucan, and other polysaccharides, have been extensively studied in fish and crustaceans [3-5] and the protective effects of some of these stimulants have been reported against WSSV infection [6]. Based on this information, we recently investigated the protective effects of dry powdered KNK-A001 on WSSV-infected kuruma shrimp. Surprisingly, shrimp fed a diet containing 0.05% KNK-A001 showed a significantly higher survival rate than shrimps fed a control diet without KNK-A001. In addition, increased haemocyte cell density was observed in the haemolymph obtained from the shrimp fed 0.05% KNK-A001, and the superoxide anion producing activity of the haemocytes

was also higher than that of the control [7]. These results suggested that KNK-A001 was a promising immunostimulant for use in shrimp farming to prevent or mitigate the impact of WSSV infection. However, the detailed mechanisms of the immunostimulatory activity of KNK-A001, especially the responsible substances, are completely unclear. As a significantly high level of mucus substances were detected in the suspension of dry-powered KNK-A001 in distilled water, we investigated the water-soluble fractions obtained from KNK-A001 and focused on the polysaccharides.

2. Materials and methods

2.1. Materials

KNK-A001 was cultured at 30 °C in a glucose-based medium originally developed by Kaneka Co., Osaka, Japan. The dry powdered KNK-A001 was prepared with a drum dryer, as previously described [7]. DEAE-Toyopearl 650S was purchased from Tosoh Co., Tokyo, Japan. The mitogen-activated protein (MAP) kinase inhibitors (PD98059, SB202190, and 600125), which are specific inhibitors for extracellular-regulated kinase (ERK), p38 MAP kinase, and c-jun N-terminal kinase (JNK), respectively, were purchased from Wako Pure Chemical Industries, Ltd (Osaka, Japan). N^{G}-Monomethyl-L-arginine acetate (L-NMMA) was obtained from Dojindo Chemical Laboratories (Kumamoto, Japan). Anti-iNOS, anti-β-actin, anti-NF-κB p65, and anti-histone H3 antibody were purchased from Merck Millipore (Billerica, MA, USA), Abcam (Cambridge, UK), Cell Signaling Technology, Inc. (Danvers, MA, USA), and BioLegend (San Diego, CA, USA), respectively. Other chemicals were of the highest grade available commercially.

2.2. Extraction, isolation, and purification of polysaccharide fractions of KNK-A001

Dry powdered KNK-A001 was suspended in distilled water at 10 mg/mL and dialyzed with an 8,000 MW cut-off against distilled water for 3 days at 4 °C to remove low molecular weight

substances. After dialysis, the suspension was autoclaved at 121 °C for 15 min to extract the hot-water soluble fractions. To remove the insoluble materials, the suspension was centrifuged at 21,600 × *g* for 30 min at 4 °C. The supernatant was applied to a column (2.5 × 40 cm) of DEAE-Toyopearl 650S previously equilibrated with distilled water. After elution with distilled water, the absorbed fractions were eluted with a linear gradient of NaCl (0–1.0 M). The sugar level in each fraction was monitored by a phenol-sulphuric acid method. To estimate the apparent molecular weight of the specific fraction (F5), the sample was applied to a column (1.6 × 93 cm) of Sepharose 4B previously equilibrated with distilled water, and eluted with distilled water. The elution was monitored by a phenol-sulphuric acid method. Dextrans of different molecular weights were used to construct the calibration curve.

2.3. Chemical composition analyses

The composition of neutral monosaccharides in each separated fraction obtained by anion-exchange chromatography was analysed with a high-performance liquid chromatography (HPLC) system (BioAssist eZ, Tosoh Co.) equipped with a PN-PAK C18 (3.0 × 75 mm) column using the ABEE method [8]. The content of phenolic compounds was estimated by the Folin-Denis method [9]. The protein level was measured by the RC DC™ protein assay kit (Bio-Rad Laboratories, Hercules, CA, USA). Fourier-transformed infrared spectrum of F5 was measured by the KBr pellet method using the Nicolet Nexus 670NT FT-IR apparatus (Thermo Fisher Scientific Inc., MA, USA).

2.4. Cell culture

RAW264.7 (mouse macrophage) cells were obtained from American Type Culture Collection (Rockville, MD, USA), and cultured in Dulbecco's modified Eagle's medium (DMEM, Wako Pure Chemical Industries, Ltd) supplemented with 10% foetal bovine serum (FBS), 100 IU/mL penicillin G, and 100 μg/mL streptomycin in a humidified atmosphere of 5% CO_2 and 95% air

at 37 °C. Adherent RAW264.7 cells were harvested by mild scraping and collected by centrifugation (270 × *g* for 3 min at 4 °C).

2.5. Cytotoxicity

The cytotoxic effect of the sample on RAW264.7 cells was measured by the 3-(4,5-dimethylthiazol-2-yl)-2,5-diphenyltetrazolium bromide (MTT) assay, as previously described [8]. In brief, adherent RAW264.7 cells (5×10^4 cells/well in 96-well plates) were incubated with varying concentrations of the sample in the growth medium for 24 h and then MTT was added to the treated cells. After 30 min of incubation, the optical density of the MTT formazan reaction product was measured at 570 nm by using a Multiskan GO scanner (Thermo Fisher Scientific Inc., MA, USA).

2.6. Nitrite assay for the estimation of nitric oxide

Adherent RAW264.7 cells (5×10^4 cells/well in 96-well plates) were incubated with the indicated concentrations of various samples for 24 h at 37 °C. After incubation, the nitrite levels in the culture medium of the treated cells were estimated by Griess assay. To examine the effects of three MAP kinase inhibitors, adherent RAW264.7 cells (5×10^4 cells/well in 96-well plates) were pre-incubated with each inhibitor at a final concentration of 10 μM for 1 h at 37 °C in the growth medium. Subsequently, F5 was added to the treated cells at a final concentration of 500 μg/mL. After 24 h incubation, the nitrite levels in the culture medium were estimated.

2.7. Enzyme-linked immunosorbent assay (ELISA)

Adherent RAW264.7 cells (5×10^4 cells/well in 96-well plates) were incubated with the indicated concentrations of various samples for 24 h at 37 °C. After incubation, TNF-α levels in the culture medium of the treated cells were estimated by ELISA, as previously described [10].

The effects of MAP kinase inhibitors on the TNF-α production were examined by the same procedure as described above in the NO production.

2.8. RNA isolation, cDNA synthesis, and reverse transcription-polymerase chain reaction (RT-PCR)

Adherent RAW264.7 cells (2×10^6 cells/dish in a 35-mm dish) were treated with each sample at a concentration of 500 μg/mL at 37 °C for 4 h. After incubation, the total RNA was extracted from the treated cells using TRIsure™ (NIPPON Genetics Co., Ltd, Tokyo, Japan) in accordance with the manufacturer's instructions. The extracted total RNA (2.5 μg) was reverse-transcribed into single-stranded cDNA by using the PrimeScript® 1st strand cDNA Synthesis Kit (Takara Bio Inc., Shiga, Japan). PCR was performed by using the GoTaq® Green Master Mix (Promega, Madison, WI, USA) and the relevant primers. The primers for the endogenous control (β-actin) and the target genes were as follows: β-actin, 5′-GGAGAAGATCTGGCACCACACC-3′ (forward) and 5′-CCTGCTTGCTGATCCACATCTGCTGG-3′ (reverse); iNOS, 5′-CAACCAGTATTATGGCTCCT-3′ (forward) and 5′-GTGACAGCCCGGTCTTTCCA-3′ (reverse). The PCR cycling parameters were as follows: 1 cycle of 70 s at 95 °C; followed by 25 cycles of 55 s at 93 °C, 45 s at 61 °C, 40 s at 72 °C; and 1 cycle of 100 s at 72 °C. Each PCR product (10 μL) was separated on 2% agarose gels containing 0.1 μg/mL ethidium bromide and observed by light capture (ATTO Co., Tokyo, Japan).

2.9. Western blot analysis

To estimate the expression level of the iNOS protein, adherent RAW264.7 cells (3×10^6 cells/dish in a 35-mm dish) were treated with F5 at a final concentration of 500 μg/mL in the growth medium at 37 °C. After a 6-h incubation period, the cells were lysed on ice with extraction buffer (10 mM HEPES, pH 7.4, 150 mM NaCl, 1 mM ethylene glycol tetraacetic

acid, 1% CHAPS, and 1% Triton™ X-100) that contained 1% protease inhibitor cocktail (Nacalai Tesque Inc., Kyoto, Japan). After 30 min, the cytosolic fraction was obtained by centrifugation at 21,600 × *g* at 4 °C for 10 min. To estimate the nuclear level of the NF-κB p65 subunit, adherent RAW264.7 cells (5×10^6 cells/dish in a 35-mm dish) were treated with F5 to a final concentration of 500 μg/mL in serum-free DMEM at 37 °C. After incubation for 1 h, the cells were washed three times with ice-cold PBS and incubated on ice with 100 μL ice-cold cytosol extraction buffer (10 mM HEPES, pH 7.9, 1.5 mM $MgCl_2$, 10 mM KCl, 0.2% Igepal® CA-630, 1 mM dithiothreitol, 20 mM β-glycerophosphate, and 1 mM sodium orthovanadate) that contained 1% protease inhibitor cocktail (Nacalai Tesque) for 25 min. The cytosolic extract was collected by centrifugation at 4,700 × *g* for 5 min at 4 °C. The nuclear pellets were resuspended in 20 μL ice-cold nuclear extraction buffer (20 mM HEPES, pH 7.9, 1.5 mM $MgCl_2$, 0.45 M NaCl, 25% glycerol, 0.2 mM ethylenediaminetetraacetic acid, and 1 mM dithiothreitol) that contained 1% protease inhibitor cocktail (Nacalai Tesque) and were incubated on ice for 25 min. After that, the nuclear extracts were obtained by centrifugation at 21,600 × *g* for 10 min at 4 °C. The extracts (containing 20 or 40 μg of protein) were subjected to 6 or 10% sodium dodecyl sulphate-polyacrylamide gel electrophoresis. The proteins were then electrophoretically transferred to a polyvinylidene difluoride membrane by using a Trans-Blot® Turbo™ Transfer System (Bio-Rad Laboratories). Each protein was analysed by western blotting using specific primary antibodies and anti-rabbit immunoglobulin G horseradish peroxidase-conjugated secondary antibodies (Merck Millipore), and visualization with Amersham™ ECL™ Prime (GE Healthcare).

2.10. Statistical analysis

All statistical analyses were performed by using GraphPad Prism 6 software (GraphPad Software, San Diego, CA, USA). A *P*-value of <0.05 was considered to be statistically significant.

3. Results and discussion

3.1. Fractionation of crude extracts of KNK-A001 by DEAE anion exchange chromatography and bioactivities of separated fractions

Hot water extracts prepared from KNK-A001 were applied to a column of DEAE anion exchange chromatography. After the elution of the unabsorbed fraction, the absorbed fractions were eluted with a linear gradient of NaCl (0–1.0 M). Based on the elution profile shown in Fig. 1, five fractions were collected (F1–F5). Table 1 shows the yield of each fraction. Based on the results of Table 1, it appeared likely that F5 and F2 were minor components of the extract of KNK-A001 relative to other fractions. To evaluate the biological activities of these fractions, the effect of each fraction at a final concentration of 1,000 μg/mL on the NO production of RAW264.7 cells was examined. As shown in Fig. 2, F5 showed potent activity, but other fractions showed no significant activity. Furthermore, F5 induced the secretion of TNF-α. F2 showed a significant but weak activity, whereas F1, F3, and F4 were inactive. The crude extract before fractionation by DEAE chromatography showed no significant activity (Fig. 2). Although the exact reason is still unclear, the crude extract might contain some kind of inhibitor or suppressor to the active fractions, and those substances might be separated by chromatography from the active fractions. Further studies are required to clarify this point. To further confirm the macrophage-stimulating activity of F5, the effects of varying concentrations of F5 were examined. As shown in Fig. 3, F5 induced NO and TNF-α in a concentration-dependent manner; significant activity was observed even at concentrations below 100 μg/mL. These results indicated that KNK-A001 contained macrophage-stimulating substances, as observed in F5, which may be partly responsible for the immunostimulatory activity of KNK-A001, as observed in previous studies [2, 7].

In contrast, it has been reported that naturally occurring polysaccharides, such as fucoidan, inhibit cell proliferation and induce apoptosis-related signal pathways in certain mammalian cell lines [11, 12]. To evaluate this possibility, the cytotoxicity of F5 on RAW264.7 cells was examined. After incubation for 24 h with varying concentrations of F5, the viabilities of the

cells were determined by MTT assay. As shown in Fig. 4, concentrations of up to 1,000 μg/mL F5 resulted in no significant cytotoxicity in RAW264.7 cells.

3.2. Structural characteristics of F2 and F5

As macrophage-stimulating activity was detected in F2 and F5, it was assumed that these fractions contained the interesting bioactive substances. To obtain information on the structural characteristics of the fractions, the chemical composition of these fractions was analysed. As shown in Table 2, the main components of these fractions were saccharides, but levels of protein and low levels of phenolic compounds were also detected in both fractions. The monosaccharide compositions of F2 and F5 were contrasting, which suggested that these were structurally unrelated substances, especially in terms of polysaccharide components. As F2 is mainly composed of glucose, it may be a kind of glucan . In contrast, F5 appears to be a complex polysaccharide or glycoprotein, composed mainly of galactose, glucose, galacturonic acid, and mannose (Table 3). The elution profile of F5 on a column of Sepharose 4B showed a slightly broad single peak (data not shown). Based on the calibration curve, the apparent molecular weight of F5 was estimated to be approximately 400 kDa.

The infrared spectra of polysaccharides show various absorption peaks owing to specific stretching vibrations that depend on the types of bonds and functional groups, which thereby provide clues for the structural characteristics. The infrared spectrum of F5 is shown in Fig. 5. The absorption peaks in the ranges of 3600–3200, 2900–2800, and approximately 1045 cm^{-1} corresponded to the stretching vibrations of O–H, C–H, and C–O, respectively. The absorption at approximately 1658 cm^{-1} may reflect the presence of carboxyl groups. These results suggested that F5 was an interesting complex polysaccharide with potent macrophage-stimulating activity. However, further investigation into the primary structure of F5 is necessary.

3.3. Intracellular signalling pathways leading to NO and TNF-α secretion in F5-treated

RAW264.7 cells

It is known that inducible NO synthase (iNOS) is the main enzyme responsible for NO production in activated macrophages. Furthermore, it has been reported that bioactive polysaccharides, such as fucoidan and ascophyllan, induced NO production from RAW264.7 cells by the upregulation of iNOS mRNA and protein expression [13, 14]. Thus, we analysed the expression levels of iNOS in RAW264.7 cells treated with F5 by PCR and western blotting. In accordance with the increase in NO levels, a significant increase in iNOS mRNA level and increased iNOS protein level was observed in F5-treated RAW264.7 cells, which were similar levels to those induced by 100 ng/mL LPS (Fig. 6A, B). The significant inhibitory effect of an iNOS inhibitor also confirmed the involvement of iNOS in NO production in F5-treated RAW264.7 cells (Fig. 6C).

The transcription factor NF-κB regulates many important biological and pathological processes [15] and is a key factor that modulates the expression of various genes involved in the immune and inflammatory responses, including iNOS and TNF-α [16-18]. Indeed, the iNOS gene promoter contains several homologous consensus sequences for the binding of NF-κB [17, 18], which is believed to be essential for iNOS transcription [19, 20]. The activation of NF-κB proceeds through the phosphorylation and degradation of the IκB-α inhibitory subunit and subsequent translocation of the p65/p50 complex into the nucleus [21]. Thus, the nuclear translocation level of p65 in F5-treated RAW264.7 cells was examined by immunoblotting. As shown in Fig. 7, the nuclear level of the p65 protein increased in F5-treated RAW264.7 cells, similar to LPS-treated cells. These results suggested that F5 was capable of activating NF-κB, which may be the main mechanism underlying the stimulation of macrophages.

In addition to the transcription factors, it has been considered that multiple intracellular pathways are implicated in the transmission of extracellular signals to the nuclei to induce iNOS gene expression [22]. It has been reported that brouw seaweed-derived sulphated polysaccharides induced protein tyrosine phosphorylation of protein kinases, protein kinase C activity, and specifically stimulated the activity of p21 activated kinase, ERK, JNK, and p38

MAPK, which leads to inflammatory cytokine secretion and urokinase-type plasminogen activator expression [23, 24]. To investigate whether MAP kinase signal pathways were involved in NO and TNF-α productions in F5-treated RAW264.7 cells, the effects of PD98059, SB202190, and SP600125, which are specific inhibitors of ERK, p38, and JNK MAP kinase, respectively, were examined at a final inhibitor concentration of 10 μM. Under these conditions, the inhibitors themselves exerted no cytotoxicity on RAW264.7 cells [25]. The results suggested that JNK and p38, but not ERK, may play an important role in NO and TNF-α productions in F5-treated RAW264.7 cells (Fig. 8). Similar to F5, our previous study on the macrophage-stimulating activities of sulphated polysaccharide ascophyllan isolated from brown seaweed *Ascophyllum nodosum* suggested that JNK and p38 but not ERK MAP kinases are mainly involved in ascophyllan-induced NO production in RAW264.7 cells [14]. Although the entire chemical structures of ascophyllan and F5 might be different each other, a MAP kinase system-mediated common intracellular signalling pathway leading to NO production may be involved in the macrophage-stimulating activities of F5 and ascophyllan. Further studies are required to clarify the exact mechanism of the involvement of the MAP kinase system in the F5-induced macrophage stimulation, but it appears likely that F5 has the ability to stimulate intracellular signalling, including the MAP kinase system, and the subsequent activation of NF-κB, which can result in the eventual secretion of NO and TNF-α.

4. Conclusion

Four fractions were obtained from the hot water extracts of KNK-A001 by anion-exchange chromatography. Among the fractions, F5 showed the most potent NO-inducing activity in the RAW264.7 mouse macrophage cell line. Analysis of the chemical structure suggested that F5 is a high molecular weight complex polysaccharide (approximately 400 kDa) mainly composed of galactose, glucose, galacturonic acid, and mannose. Reverse transcription polymerase chain reaction (RT-PCR) and western blot analysis revealed that the expression of both mRNA and protein levels of inducible NO synthase (iNOS) in F5-treated

RAW264.7 cells were increased compared with the control. A significant increase in the nuclear translocation of the p65 subunit of NF-κB was observed in F5-treated RAW264.7 cells. The analysis using MAP kinase inhibitors suggested that JNK and p38 MAP kinase were involved in F5-induced NO and TNF-α productions. F5 also induced the secretion of TNF-α from RAW264.7 cells in a concentration-dependent manner in the range from 7.8–500 μg/mL. Our results suggested that F5 may be a novel complex polysaccharide with potent macrophage-stimulatory activity, although further studies on the structure-activity relationships of F5 are required.

Acknowledgements

This work was supported in part by a Grant-in-Aid (15K07580) for Scientific Research from the Ministry of Education, Culture, Sports, Science and Technology of Japan, a fund from Nagasaki University Major Research Project (Research Initiative for Adaptation to Future Ocean Change), and a project funded by Grant-in-Aid for Japan Society for the Promotion of Science (JSPS) Fellows to M. Ueno. This work was also supported by Korea Basic Science Institute (C37290) partly and the National Research Foundation of Korea (NRF-2017R1A2B4005582).

References

[1] Y. Sugiyama, M. Ueno, C.G.P. Satuito, K. Yamashita, K. Yamaguchi, T. Oda. Aquaculture Sci.61 (2013) 389-394.

[2] M. Ueno, Z. Jiang, R. Abu, K. Yamashita, K. Yamaguchi, T. Oda. Jpn. J. Food Chem. 22 (2015) 63-69.

[3] V.J. Smith, J.H. Brown, C. Hauton. Fish Shellfish Immunol. 15 (2003) 71-90.

[4] M. Sakai. Aquaculture 172 (1999) 63-92.

[5] Y.L. Song, C.C. Huang. In: Immunology and pathology eds. by M. Fingerman, R.

Nagabhushanam. Enfield, New Hampshire, USA: Science Publishers, Inc. 5 (1999) 173-88.
[6] A. Namikoshi, J.L. Wu, Y. Yamashita, T. Nishizawa, T. Nishioka, M. Arimoto. Aquaculture 229 (2004) 25-35.
[7] M. Ueno, T. Itami, K. Yamashita, T. Oda. Aquaculture Sci. 64 (2016) 201-204.
[8] S. Isaka, K. Cho, S. Nakazono, R. Abu, M. Ueno, D. Kim, T. Oda, Int. J. Biol. Macromol. 74 (2015) 68-75.
[9] Y. Niwano, E. Sato, M. Kohno, Y. Matsuyama, D. Kim, T. Oda. Biosci. Biotechnol. Biochem. 71 (2007) 1145-1153.
[10] M. Ueno, K. Cho, S. Nakazono, S. Isaka, R. Abu, S. Takeshita, K. Yamaguchi, D. Kim, and T. Oda. Biosci. Biotechnol. Biochem. 79 (2015) 1787-1793.
[11] E.J. Kim, S.Y. Park, J.Y. Lee, J.H. Park. B.M.C. Gastroenterology 10 (2010) 96.
[12] J.O. Jin, M.G. Song, Y.N. Kim, J.I. Park, J.Y. Kwak. Mol Carcinog. 49 (2010) 771-782.
[13] T. Nakamura, H. Suzuki, Y. Wada, T. Kodama, T. Doi. Biochem. Biophys. Res. Commum. 343 (2006) 286-294.
[14] Z. Jiang, T. Okimura, K. Yamaguchi, T. Oda. Nitric Oxide 25 (2011) 407-415.
[15] S. Fujioka, J. Niu, C. Schmidt, G.M. Sclabas, B. Peng, T. Uwagawa, Z. Li, D.B. Evans, J.L. Abbruzzese, P.J. Chiao. Mol. Cell Biol. 24 (2004) 7806-7819.
[16] S. Rudders, J. Gaspar, R. Madore, C. Voland, F. Grall, A. Patel, A. Pellacani, M.A. Perrella, T.A. Libermann, P. Oettgen. J. Biol. Chem. 276 (2001) 3302–3309.
[17] K. Cieslik, Y. Zhu, K.K. Wu. J. Biol. Chem. 277 (2002) 49304-49310.
[18] A.K. Lee, S.H. Sung, Y.C. Kim, S.G. Kim. Br. J. Pharmacol. 139 (2003) 11-20.
[19] Q.W. Xie, R. Whisnant, C. Nathan. J. Exp. Med. 177 (1993) 1779-1784.
[20] M.J.M. Diaz-Guerra, M. Velasco, P. Martin-Sanz, L. Bosca. J. Biol. Chem. 271 (1996) 30114-30120.
[21] T. Wang, X. Zhang, J. J. Li. Int. Immunopharmacol. 2 (2002) 1509-1520.
[22] R. Korhonen, A. Lahti, H. Kankaanranta, E. Moilanen. Curr. Drug Targets Inflamm. Allergy 4 (2005) 471-479.
[23] H.Y. Hsu, D.P. Hajjar, K.M. Khan, D.J. Falcone. J. Biol. Chem. 273 (1998) 1240-1246.

[24] H.Y. Hsu, S.L. Chiu, M.H. Wen, K.Y. Chen, K.F. Hua. J. Biol. Chem. 276 (2001) 28719-28730.
[25] D. Kim, Y. Yamasaki, Z. Jiang, Y. Nakayama, T. Yamanishi, K. Yamaguchi, T. Oda. Acta Biochim. Biophys. Sin. 43 (2011) 52-60.

Table 1. Yield of each fraction obtained from DEAE anion exchange chromatography.

	F1	F2	F3	F4	F5
Yield[a]	25.8	4.5	16.7	48.5	4.5

[a] w/w% of dry weight.

Table 2. Chemical composition of F2 and F5

	F2	F5
Sugar[a]	40	45
Protein[b]	3	26
Phenolic compounds[c]	0.44	2.9

[a] The values were estimated by the phenol-sulphuric acid method.

[b] The values were estimated by the RC DC™ protein assay.

[c] The values were estimated by the Folin-Denis method.

Table 3. Composition of monosaccharides of F2 and F5

	F2	F5
Glucuronic acid	ND[a]	2.4
Galacturonic acid	ND	14
Galactose	4.2	33
Mannose	4.0	7.0
Glucose	84	16.2
Arabinose	1.0	5.0
Ribose	ND	0.7
Xylose	2.7	2.8
N-Acetyl-glucosamine	ND	0.2
Rhamnose	8.1	8.0

[a] ND, not detectable.

Figure legends

Fig. 1. The elution profile of hot water extracts prepared from KNK-A001 on DEAE anion exchange chromatography. The extract from KNK-A001 was applied to a column (2.5 × 40 cm) of DEAE-Toyopearl 650S previously equilibrated with distilled water and eluted with distilled water. The absorbed fractions were eluted with a linear gradient of NaCl (0–1.0 M). The sugar level in each fraction was monitored by the phenol-sulphuric acid method.

Fig. 2. The effects of the crude extract and separated fractions obtained by DEAE anion exchange chromatography on RAW264.7 cells with respect to NO induction and TNF-α secretion. Adherent RAW264.7 cells (5×10^4 cells/well in 96-well plates) were incubated with 1 mg/mL of each sample for 24 h. After the incubation, NO and TNF-α levels in the supernatants of the treated cell were estimated by Griess assay and ELISA, respectively, as described in the Methods. The columns indicate the mean ± S.D. of triplicate measurements.

Fig. 3. The effects of F5 obtained by DEAE anion exchange chromatography on RAW264.7 cells to induce NO and TNF-α secretion. Adherent RAW264.7 cells (5×10^4 cells/well in 96-well plates) were incubated with the indicated concentrations of F5 for 24 h. After incubation, the NO and TNF-α levels in the supernatant of the treated cells were estimated by Griess assay and ELISA, respectively, as described in the Method. The columns indicate the mean ± S.D. of quadruplicate measurements.

Fig. 4. The cytotoxic effects of F5 on RAW264.7 cells. Adherent RAW264.7 cells (5×10^4 cells/well in 96-well plates) were incubated with the indicated concentrations of F5 for 24 h. After incubation, the cell viabilities were estimated by MTT assay as described in the Methods. Each point indicates the mean ± S.D. of triplicate measurements.

Fig. 5. The infrared spectrum of F5.

Fig. 6. The levels of iNOS mRNA and protein in F5-treated RAW264.7 cells and the effects of L-NMMA on F5-induced NO secretion. (A) After 4 h of incubation with 500 μg/mL F5, iNOS mRNA levels in RAW264.7 cells were analysed by RT-PCR as described in the Methods. (B) After incubation for 6 h with 500 μg/mL F5, iNOS protein levels in RAW264.7 cells were analysed by western blotting, as described in the Methods. (C) Adherent RAW264.7 cells were pre-incubated with L-NMMA (100 μM) for 1 h and F5 (500 μg/mL) was added to the cells. After incubation for 24 h, the nitrite levels in the cultured supernatants were estimated by Griess assay, as described in the Methods. Each column indicated the mean ± S.D. of quadruplicate measurements.

Fig. 7. The effects of F5 on the nuclear translocation of the NF-κB p65 subunit in RAW264.7 cells. After incubation for 1 h with 500 μg/mL F5, the nuclear level of the NF-κB p65 subunit in the treated cells was analysed by western blotting, as described in the Methods.

Fig. 8. The effects of MAP kinase inhibitors on F5-induced NO (A) and TNF-α (B) productions from RAW264.7 cells. Adherent RAW264.7 cells were pre-incubated with 10 μM of each MAP kinase inhibitor for 1 h and F5 (500 μg/mL) was added to the cells. After incubation for 24 h, the nitrite and TNF-α levels in the cultured supernatants were estimated by Griess assay and ELISA as described in the Methods, respectively. Each column indicated the mean ± S.D. of quintuplicate measurements (A) or triplicate measurements (B).

Figure 1

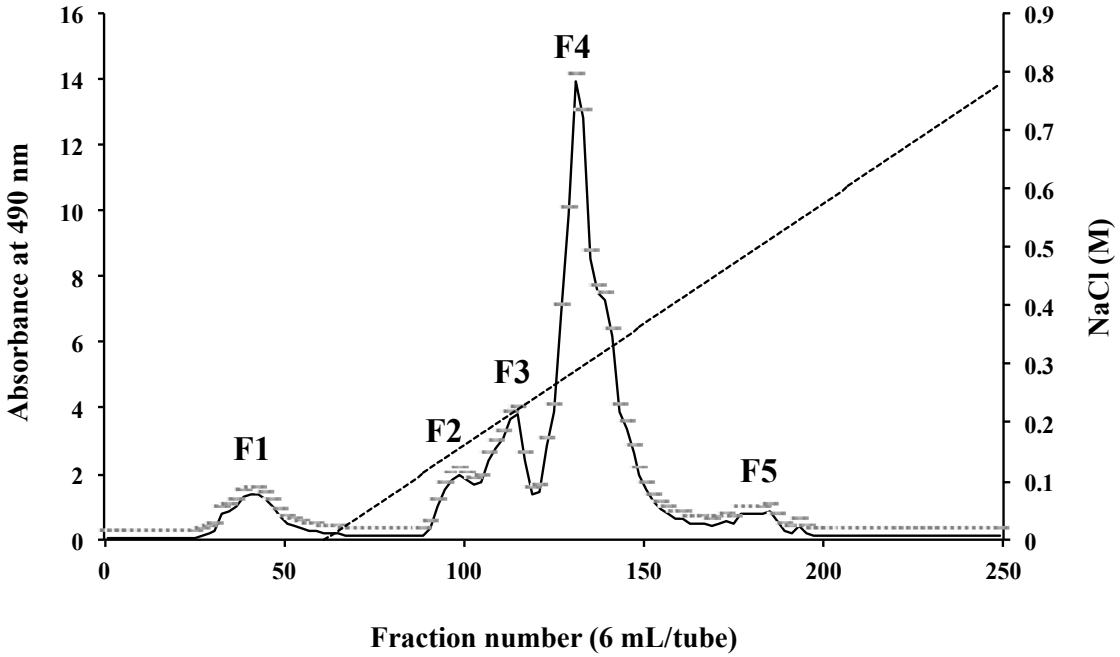
Absorbance at 490 nm
NaCl (M)
Fraction number (6 mL/tube)
F1
F2
F3
F4
F5
0
2
4
6
8
10
12
14
16
0
0.1
0.2
0.3
0.4
0.5
0.6
0.7
0.8
0.9
0
50
100
150
200
250

Figure 2

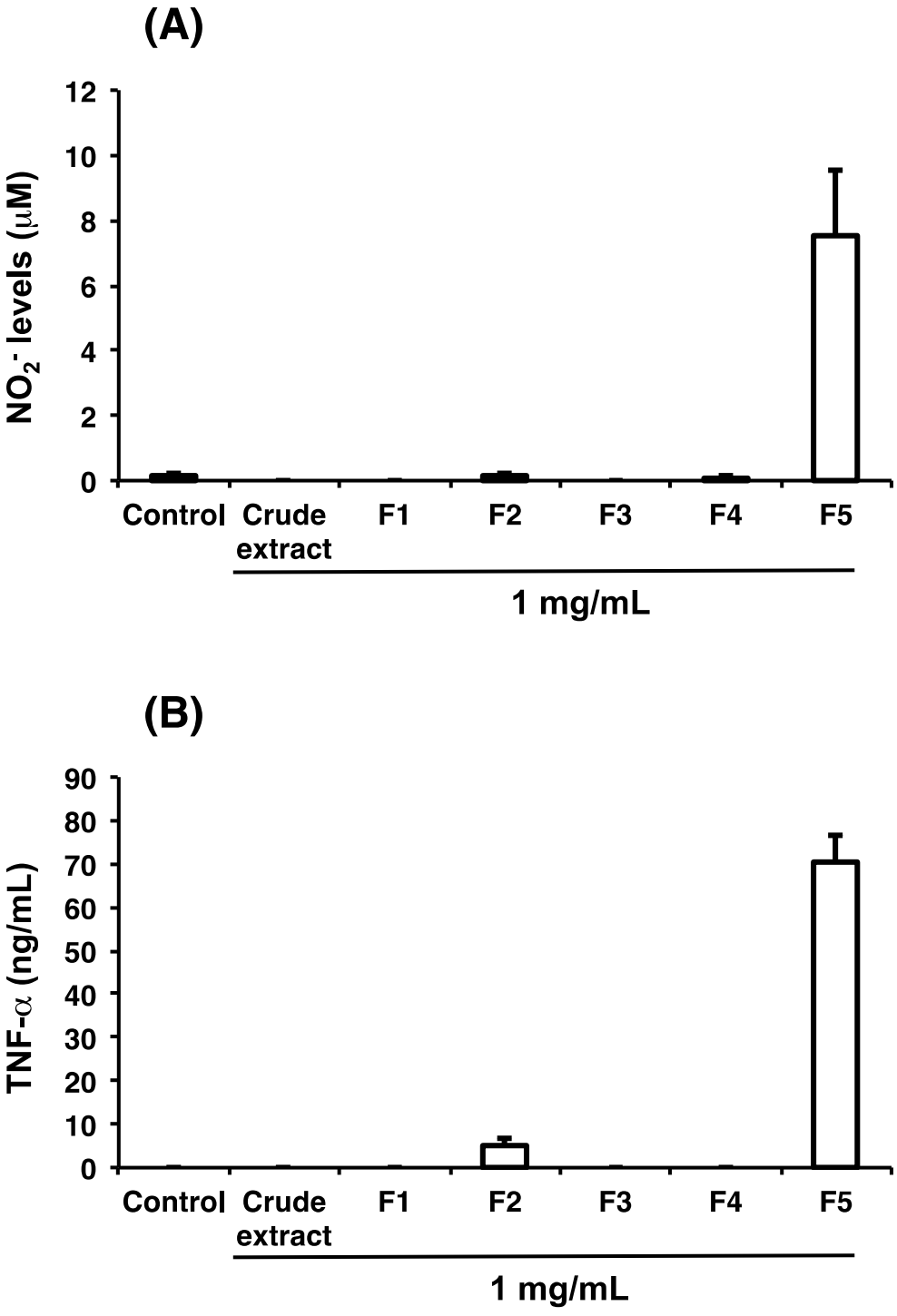
(A)
12
10
8
6
4
2
0
NO_2^- levels (μM)
Control
Crude extract
F1
F2
F3
F4
F5
1 mg/mL
(B)
90
80
70
60
50
40
30
20
10
0
TNF-α (ng/mL)
Control
Crude extract
F1
F2
F3
F4
F5
1 mg/mL

Figure 3

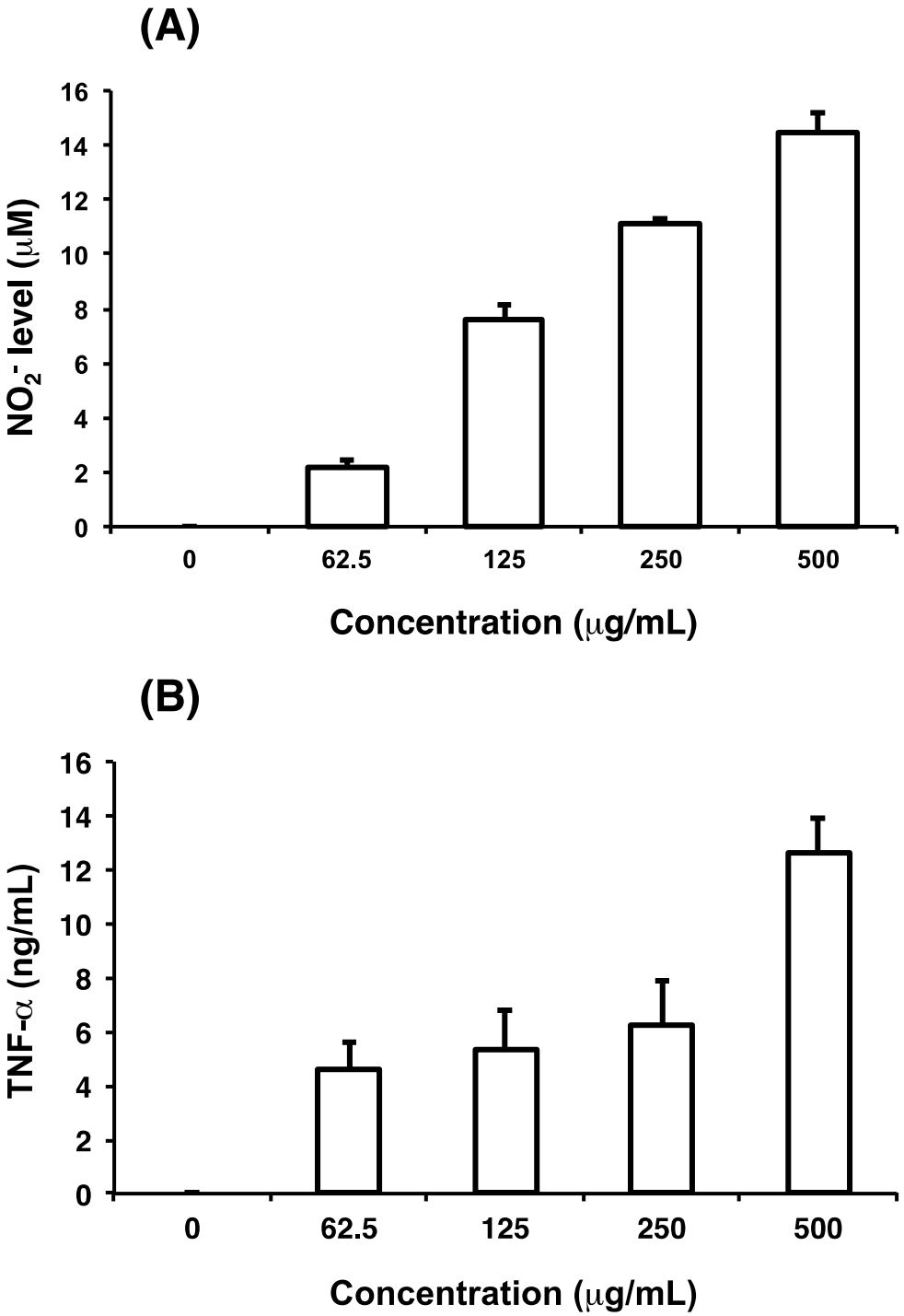
(A)
16
14
12
10
8
6
4
2
0
NO_2^- level (μM)
0
62.5
125
250
500
Concentration (μg/mL)
(B)
16
14
12
10
8
6
4
2
0
TNF-α (ng/mL)
0
62.5
125
250
500
Concentration (μg/mL)

Figure 4

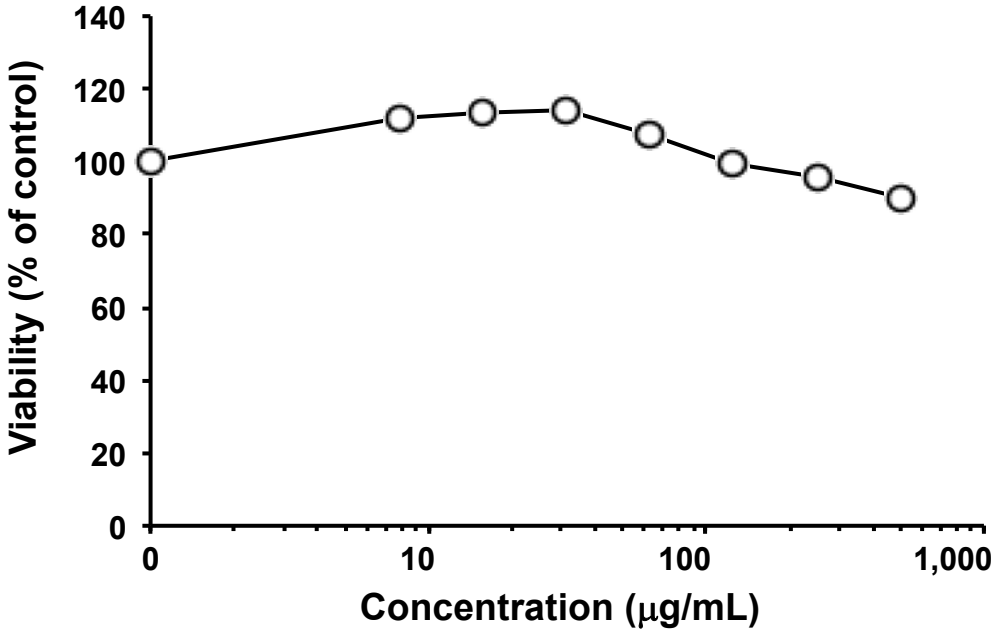
Viability (% of control)
140
120
100
80
60
40
20
0
0
10
100
1,000
Concentration (μg/mL)

Figure 5

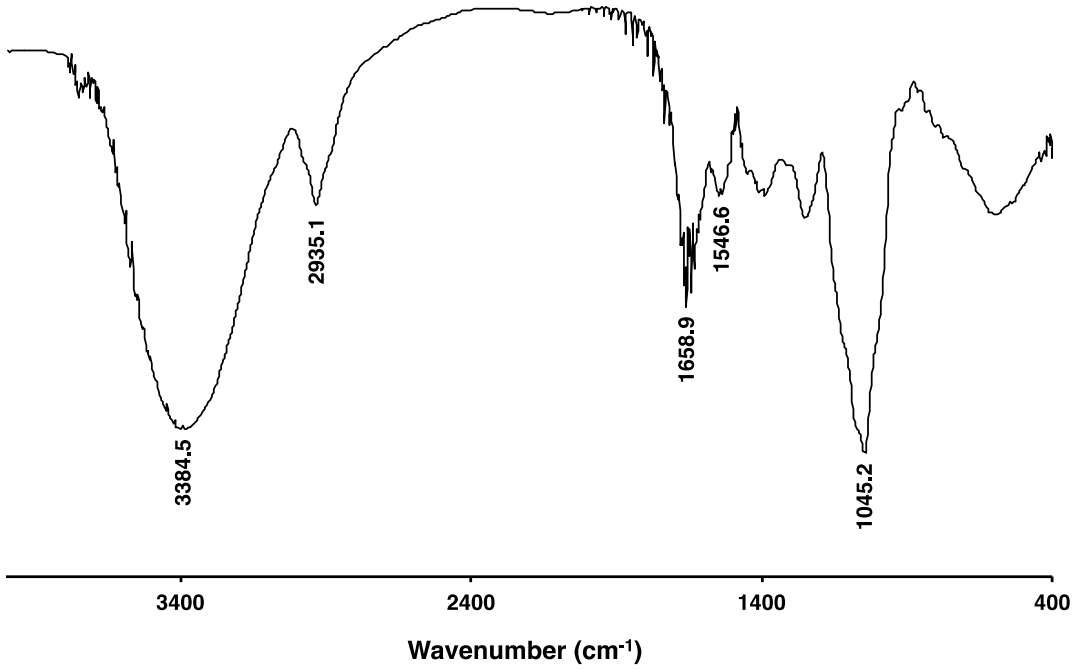
3384.5
2935.1
1658.9
1546.6
1045.2
3400
2400
1400
400
Wavenumber (cm-1)

Figure 6

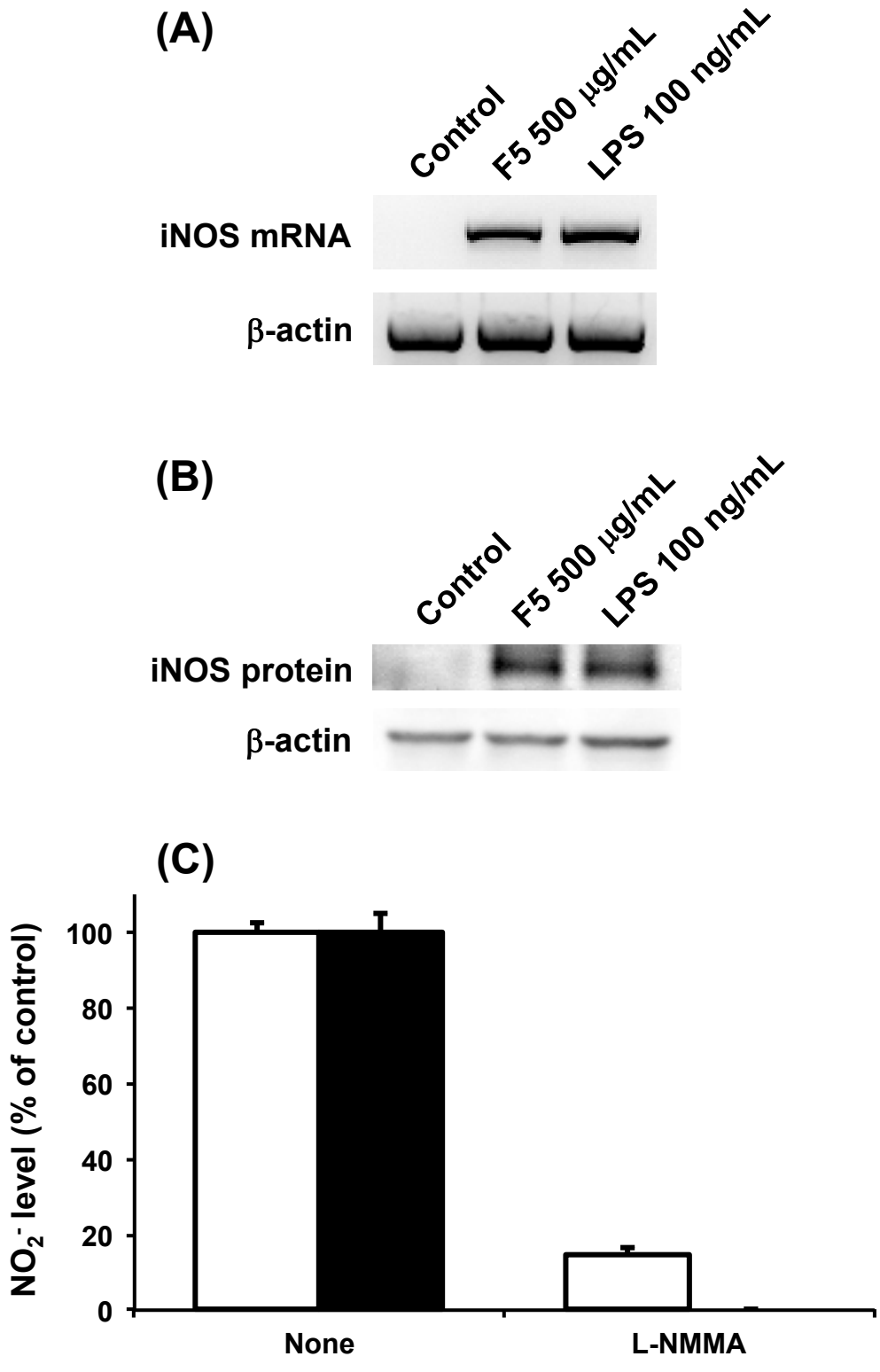
(A)
Control
F5 500 μg/mL
LPS 100 ng/mL
iNOS mRNA
β-actin
(B)
Control
F5 500 μg/mL
LPS 100 ng/mL
iNOS protein
β-actin
(C)
NO_2^- level (% of control)
100
80
60
40
20
0
None
L-NMMA

Figure 7

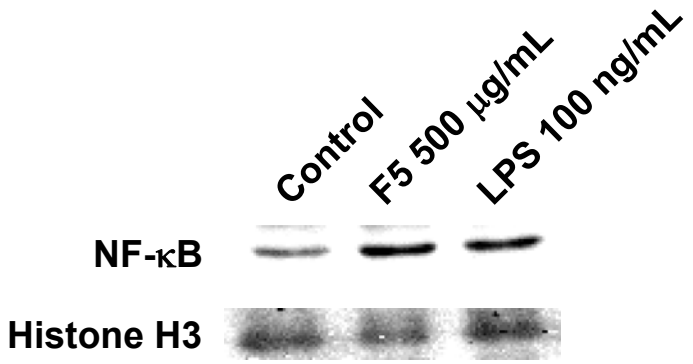

Figure 8

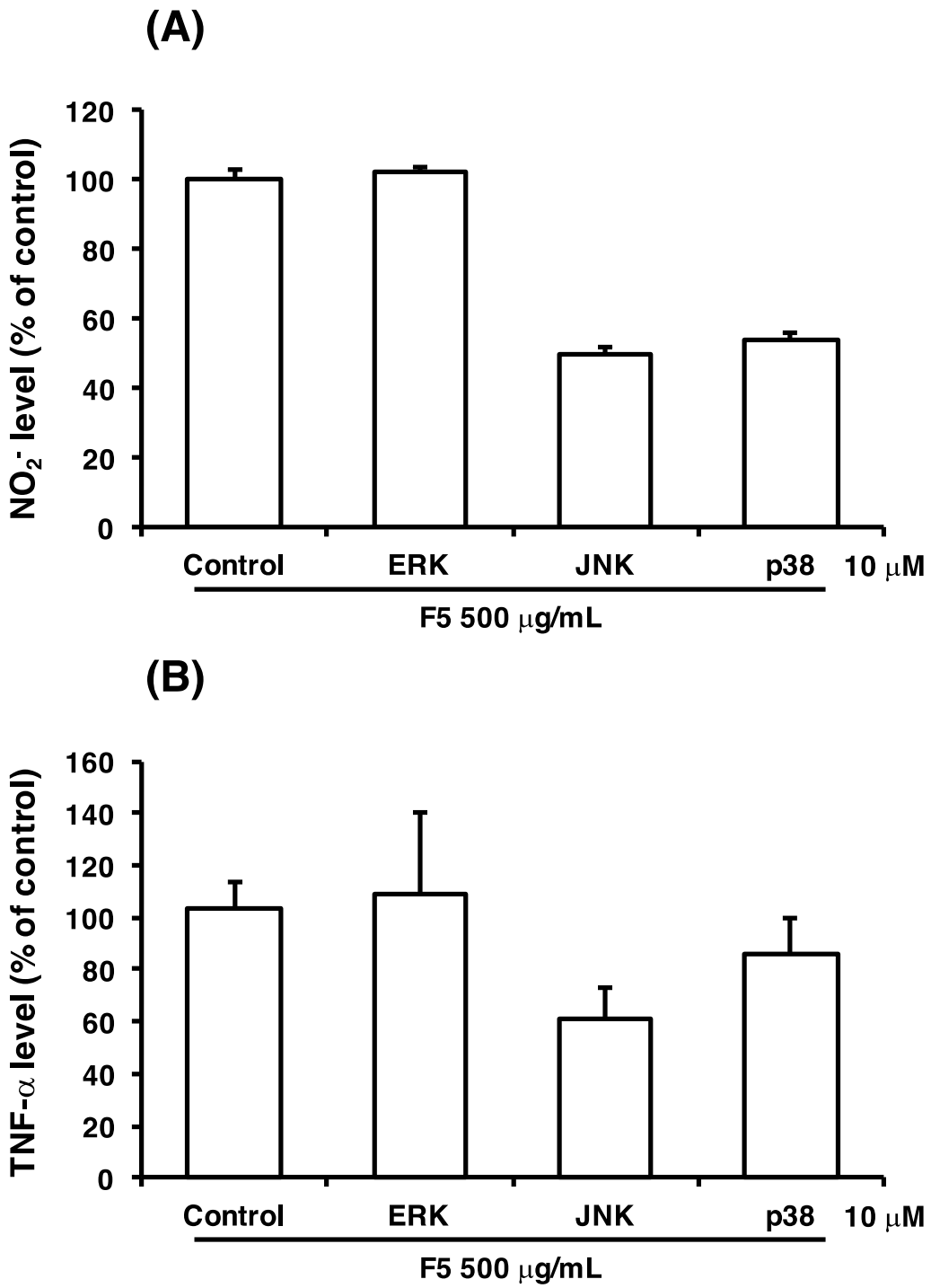
(A)
NO_2^- level (% of control)
120
100
80
60
40
20
0
Control
ERK
JNK
p38
10 μM
F5 500 μg/mL
(B)
TNF-α level (% of control)
160
140
120
100
80
60
40
20
0
Control
ERK
JNK
p38
10 μM
F5 500 μg/mL